

# 1 A tipping point in cancer-immune dynamics leads to divergent immunotherapy responses 2 and hampers biomarker discovery

Jeroen H.A. Creemers<sup>1,4</sup>, Willem J. Lesterhuis<sup>3</sup>, Niven Mehra<sup>2</sup>, Winald R. Gerritsen<sup>2</sup>,  
Carl G. Figgdr<sup>1,4</sup>, I. Jolanda M. de Vries<sup>1</sup>, Johannes Textor<sup>1,5\*</sup>

- 1) Department of Tumor Immunology, Radboud Institute for Molecular Life Sciences; Radboudumc, Nijmegen, The Netherlands
  - 2) Department of Medical Oncology, Radboudumc, Nijmegen, The Netherlands
  - 3) School of Biomedical Sciences and Telethon Kids Institute, University of Western Australia, Perth, Australia
  - 4) Oncode Institute, Nijmegen, The Netherlands
  - 5) Data Science Department, Institute for Computing and Information Sciences, Radboud University, Nijmegen, The Netherlands

\* Corresponding author:

Dr. J. Textor

17 Department of Tumor Immunology, Radboud Institute for Molecular Life Sciences, Radboudumc  
18 Geert Grooteplein 26, 6500 HB Nijmegen (P.O. Box 9101), The Netherlands  
19 E-mail: [johannes.textor@radboudumc.nl](mailto:johannes.textor@radboudumc.nl)

## ABSTRACT

## Background

23 In the field of immuno-oncology, predicting treatment response or survival of cancer patients remains  
24 a challenge. Efforts to overcome these challenges focus mainly on the discovery of new biomarkers.  
25 Owing to the complexity of cancers and their tumor microenvironment, only a limited number of  
26 candidate biomarkers eventually enters clinical practice, despite advances in cellular and molecular  
27 approaches.

## Methods

29 A computational modeling approach based on ordinary differential equations was used to simulate  
30 the fundamental mechanisms that dictate tumor-immune dynamics and show its implications on  
31 responses to immune checkpoint inhibition (ICI) and patient survival. Using *in silico* biomarker  
32 discovery trials, we extracted fundamental principles underlying the success rates of biomarker  
33 discovery programs.

## Results

35 Our main finding is the prediction of a tipping point – a sharp state transition between immune control  
36 and immune evasion – that follows a strongly non-linear relationship between patient survival and  
37 both immunological and tumor-related parameters. In patients close to the tipping point, ICI therapy  
38 may lead to long-lasting survival benefits, whereas patients far from the tipping point may fail to  
39 benefit from these potent treatments.

## Conclusion

These findings have two important implications for clinical oncology. First, the apparent conundrum that ICI induces substantial benefits in some patients yet completely fails in others could be, to a large extent, explained by the presence of a tipping point. Second, predictive biomarkers for immunotherapy should ideally combine both immunological and tumor-related markers, as the distance of a patient' status from the tipping point cannot, in general, be reliably determined from solely one of these. The notion of a tipping point in cancer-immune dynamics could help to optimize strategies in biomarker discovery to ensure accurate selection of the right patient for the right treatment.

NOTE: This preprint reports new research that has not been certified by peer review and should not be used to guide clinical practice.

## 50 INTRODUCTION

51 Immunotherapies are revolutionizing clinical care for cancer patients. The most widely used approach,  
52 immune checkpoint inhibition (ICI), can lead to long-term survival benefits in patients with advanced  
53 melanoma (1), lung cancer (2), and renal cell carcinoma (3). However, not all patients benefit from ICI  
54 therapy, and adequate predictions of treatment response have proven elusive so far (4, 5). Efforts to  
55 improve these predictions focus mainly on discovering biomarkers in aberrant molecular pathways  
56 within the tumor microenvironment that drive immunosuppression and therapeutic resistance (6, 7).  
57 These include genomic alterations in oncogenic drivers, the absence of tumor-specific antigens, and  
58 the presence of immunosuppressive molecules or cells (8, 9). Despite substantial efforts, only a limited  
59 fraction (according to one estimate, <1% (10)) of proposed cancer biomarkers find their way into the  
60 clinical practice. These apparent challenges in identifying biomarkers for immunotherapy and  
61 translating them into clinical practice could be a consequence of the inherent complexity of cancers  
62 and their interaction with the immune system.

63 To unravel the complexities of cancers and their treatments, researchers have adopted mathematical  
64 and computational approaches to complement laboratory research. A plethora of modeling  
65 approaches are available, ranging from simple one-variable equations to complex spatial agent-based  
66 simulation models. *In silico* modeling has contributed to fundamental insights into tumor growth and  
67 cancer progression (11-13), tumor-immune control (e.g., neoantigen prediction as targets for  
68 immunotherapy) (14), identification of tumor-associated genes (15), verification of treatment-related  
69 safety concerns such as hematological toxicity (16), prediction of treatment responses to chemo- and  
70 immunotherapy (17-19), investigation of drug-induced resistance (20), and timing of anti-cancer  
71 treatments (21-23). In the context of disease course dynamics, ordinary differential equation (ODE)  
72 models have proven useful over the years. ODE models follow the principle that a model should be “as  
73 simple as possible but not simpler”. Based on plausible biological assumptions, they aim to reduce the  
74 complex reality of the modeled system to its bare essentials to enable investigation of critical  
75 underlying dynamics. For instance, Fassoni *et al.* used ODE models to predict that dose de-escalation  
76 of tyrosine kinase inhibitors targeting the oncogenic protein BCR-ABL1 in patients with chronic myeloid  
77 leukemia (chronic phase) does not lead to worse long-term outcomes (24). The recent results of the  
78 DESTINY trial support this prediction (25).

79 In this study, we investigate the consequences of tumor-immune dynamics on patients’ responses to  
80 ICI and survival with an ODE model. Our model reveals a tipping point within tumor-immune dynamics  
81 – a critical threshold for survival culminating in an all-or-nothing principle – that has profound  
82 implications for a patient’s disease course and outcome. We show how the presence of such a tipping  
83 point alone robustly induces heterogeneous immunotherapy treatment outcomes, and how this  
84 complicates the search for both prognostic and predictive biomarkers.

85 **METHODS**

86 **Capturing core mechanisms of the tumor microenvironment in a mathematical model**

87 We constructed a mathematical model based on a system of ordinary differential equations (ODE) to  
88 capture essential interactions between cancerous cells and lymphocytes in the tumor  
89 microenvironment. Our model represents tumorigenesis in patients, starting with the malignant  
90 transformation of a single cell.

91 The model describes the following processes: (1) conversion of naive T cells into antigen-specific  
92 effector T cells in lymph nodes; (2) the clonal expansion of effector T cells in the lymph nodes; (3)  
93 tumor growth; (4) subsequent attraction of tumor-infiltrating lymphocytes; and (5) formation of  
94 tumor-immune cell complexes to facilitate tumor cell killing. Below we describe the model; a  
95 mathematical formulation containing the model equations is provided as Supplementary Information.

96 Tumor growth is represented by the generalized exponential model proposed by Mendelsohn (26),  
97 meaning that at each time interval, a fraction of tumor cells divide. The dividing fraction decreases as  
98 the tumor burden increases since substantial parts of a larger tumor mass, such as the necrotic core,  
99 are no longer able to proliferate. During tumor development, T cells are produced in the lymph nodes.  
100 This process starts with the conversion of naive T cells (i.e., not activated antigen-specific) into antigen-  
101 specific effector T cells at a rate proportional to the tumor burden. Effector T cells expand clonally and  
102 migrate into the tumor microenvironment, where they form tumor-immune complexes (i.e., an  
103 immune cell attached to a tumor cell). Within these complexes, T cells kill the tumor cells.

104 The killing rate expression is derived from the Michaelis-Menten kinetics for enzyme-substrate  
105 interaction with a quasi-steady-state approximation, as described by Borghans *et al.* (27). Given that  
106 complex formation and dissociation occur on a time scale several orders of magnitude smaller than  
107 the time scale for tumor growth, this approximation states that this process can be regarded as a  
108 constant process. Further simplification of the killing rate expression using the Padé approximation  
109 yields the double saturation killing rate of T cells (27). T cells follow a ‘monogamous killing’ strategy,  
110 meaning that one T cell interacts with one tumor cell at a time (27, 28). In addition, T cells die and exit  
111 the system at a fixed rate.

112

113 **Simulation parameters**

114 The simulation parameters are listed in Table 1.

115 *Table 1: Simulation parameters in ODE model*

Symbol	Parameter (dimension)	Default value (range <sup>a</sup> )
$\rho$	Tumor growth rate (cells day <sup>-1</sup> )	1 (0-7)
$\xi$	Relative killing rate	0.001 (0-0.05)
$h$	Michaelis constant (cells)	571
$\delta$	Death rate of immune cells (cells day <sup>-1</sup> )	0.019 (29)

$\alpha$	Conversion rate of naive T cells into specific T cells	0.0025
$p_s$	Total production rate of effector T cells from lymph nodes (cells day <sup>-1</sup> )	1
$m_s$	Migration rate from lymph node to tumor microenvironment	1

116 <sup>a</sup>: if not fixed

117

118 The parameters were chosen to mimic realistic *in vivo* intercellular behavior. The rationale for the  
119 choice of each parameter is explained below.

120 In a human adult, an estimated repertoire of approximately  $10^{10}$  -  $10^{11}$  naive CD8<sup>+</sup> T cells is present (30,  
121 31). Naive CD8<sup>+</sup> T cells need to be primed to become activated effector T cells. The CD8<sup>+</sup> T cell precursor  
122 frequency – the frequency at which any given peptide-MHC complex is recognized by naive antigen-  
123 specific CD8<sup>+</sup> T cells – is on the order of 1 : 100.000 (30). Priming should be limited primarily to naive  
124 CD8<sup>+</sup> T cells in one of the tumor areas draining lymph nodes. A human body contains  $\pm$ 600 lymph  
125 nodes. At steady states, roughly 40% of all lymphocytes reside in lymph nodes, meaning that 40.000  
126 naive T cells ( $\approx$  70 naive CD8<sup>+</sup> T cells per lymph node) can be primed (32, 33). We assume that priming  
127 occurs primarily in the tumor-draining lymph node station (per station harboring around 20 lymph  
128 nodes (34)), leading to an optimal priming rate of 1400 T cells per day. Considering that DCs might  
129 present multiple epitopes and antigens, and that T cell priming *in vivo* might occur suboptimally, we  
130 set a priming rate of at most 2500 cells per day. The order of magnitude of these priming rates  
131 corresponds to priming rates found in chronic infectious diseases (35). Due to evasive mechanisms,  
132 anti-tumor immunity is a more dormant process than an immune response to infections (36).  
133 Therefore, we scaled the priming rate with tumor size (Supplementary Information), which translates  
134 into a maximum production of  $10^6$  antigen-specific CD8<sup>+</sup> T cells per day via clonal expansion. Next, we  
135 assume that all antigen-specific effector T cells migrate into the tumor microenvironment to interact  
136 with tumor cells (i.e., complex formation).

137 Complex formation and dissociation rates are described by ‘the Michaelis constant’, which we derived  
138 from literature (28). The Michaelis constant describes the ratio between complex formation and  
139 dissociation.

140 The killing rate of effector T cells has been investigated mainly in the context of infectious disease. In  
141 their review (37), Halle *et al.* discuss discrepancies between *in vitro* and *in vivo* killing rates of effector  
142 T cells. Dependent on the context, killing rates of effector T cells vary from 1 target per 5 minutes to  
143 0-10 targets per day (37), but tumor cells are considered difficult to kill. Extensive variation in  
144 experimental *in vivo* *per capita* killing rates (i.e., the number of cells killed by an effector T cell per unit  
145 of time) complicates the selection of a default fixed killing parameter. Therefore, we investigated T cell

146 dynamics over a range of overall killing rates as described using the monogamous killing regime in a  
147 double saturation model by Gadhamsetty *et al.* (28). The double saturation model ensures that the  
148 killing rate saturates with respect to the tumor cell and the effector cell densities. Consequently, our  
149 model's maximum per capita killing rate is  $2.5 \text{ cells}^{-1} \text{ day}^{-1}$ : one T cell can kill at most 2.5 tumor cells  
150 per day, provided there are abundant target cells available and there is no competition with other T  
151 cells. The default tumor growth rate is one cell day $^{-1}$ , but we varied this parameter extensively in our  
152 simulations. Taken together, our default parameter values led to simulations of disease courses with  
153 realistic survival times in patients with malignancies and matched the order of magnitude of tumor  
154 growth rates as reported by others (38).

155

## 156 **Patient simulations**

157 We simulated tumor development in patients up to a maximum of 5 years. Note that depending on  
158 emergent tumor-immune dynamics, simulated patients may not reach the overall survival endpoint  
159 during this interval. Each time step in the simulation corresponded to one day. At baseline, one tumor  
160 cell and a pool of  $10^6$  naïve tumor-specific T cells are present in a patient. Activated effector T cells are  
161 absent. We defined the time of diagnosis as the time at which the tumor burden exceeded  $65 * 10^8$   
162 cells and became clinically apparent. This cut-off corresponds to the assumption that a tumor with a  
163 volume of  $1 \text{ cm}^3$  contains  $10^8$  tumor cells (39) and that several primary tumors (e.g., lung cancer, colon  
164 carcinoma, and renal cell carcinoma) are diagnosed as spherical structures with a median diameter of  
165 approximately 5 cm (40-42). The 'lethal' tumor burden of patients in these simulations is estimated at  
166  $10^{12}$  cells, corresponding to a total tumor mass of approximately  $22 * 22 * 22 \text{ cm}^3$ .

167

## 168 **Model implementation**

169 We implemented our ODE model in C++. The Boost library 'odeint' was used to solve the system of  
170 ordinary differential equations (43). The code is available at GitHub:  
171 <https://github.com/jeroencreemers/tipping-point-cancer-immune-dynamics>. Analyses and  
172 visualizations were performed in R.

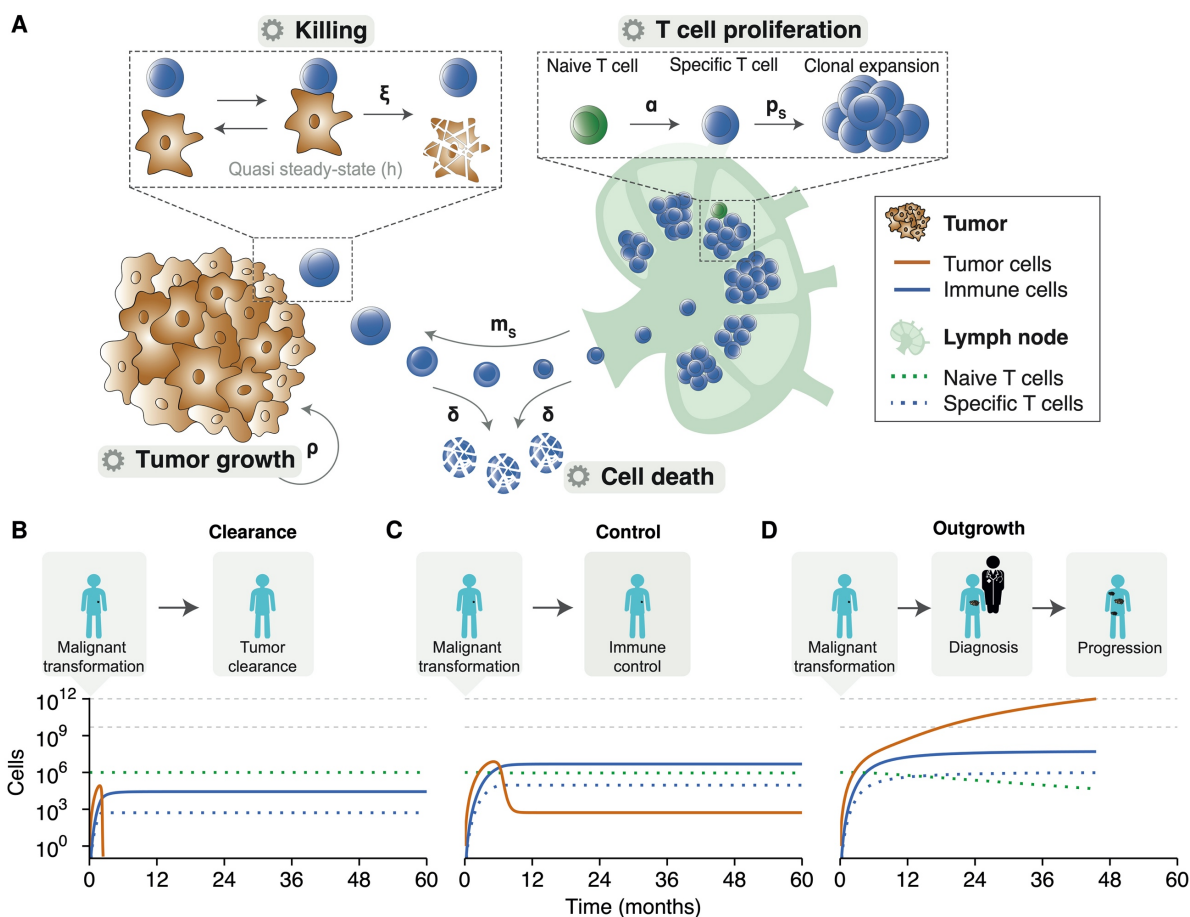
173

174

175 **RESULTS**

176 **Modeling tumor-immune dynamics yields realistic disease trajectories**

177 To investigate the consequences of tumor-immune dynamics on the survival kinetics of patients, we  
178 used a computational modeling approach. We aimed to capture the interplay between tumor- and  
179 immune cells in the tumor microenvironment and simulate tumor growth in patients (see Methods).  
180 Our ODE model captured four essential processes in anti-tumor immunity: priming of naive antigen-  
181 specific CD8<sup>+</sup> T cells, clonal expansion of effector T cells in lymph nodes, tumor growth leading to  
182 effector T cell attraction into the tumor microenvironment, and formation of tumor-immune cell  
183 complexes to enable tumor cell killing (Fig. 1A).



185 **Figure 1: An in silico model of the tumor microenvironment generates realistic and modifiable disease courses of cancer**  
186 **patients. (A)** The ODE model describes fundamental processes in the tumor microenvironment. Parameters:  $\alpha$  = naive T cell  
187 priming rate,  $\delta$  = effector T cell death rate,  $\xi$  = effector T cell killing rate,  $\rho$  = tumor growth rate,  $p_s$  = effector T cell proliferation  
188 rate, and  $m_s$  = effector T cell migration rate. **(B)** An effective anti-tumor immune response can eradicate tumor cells before  
189 the clinical manifestation of a tumor. **(C)** After an initial state in which the tumor outpaces the immune system, the immune  
190 system can suppress tumor growth and controls it in a subclinical state. **(D)** The natural course of disease for a clinically  
191 apparent tumor. An initial malignant transformation is followed by tumor growth until clinical diagnosis. Despite the  
192 activation of adaptive immunity, the tumor prevails. A stage of progressive disease follows, ultimately culminating in cancer-  
193 related death. The horizontal grey lines indicate (from bottom to top): the tumor burden at diagnosis and the tumor burden  
194 at death, respectively. Simulation parameters are added in Supplementary Table 1.

196 We simulated tumor development from malignant transformation of a single cell, via clinical detection  
197 of a tumor, to advanced disease and possibly death. Depending on the tumor growth and the cytotoxic  
198 capacity of effector T cells, the ‘time to clinical manifestation’ and overall survival varied. Despite this  
199 variation, our simulations consistently showed three possible outcomes: 1) effector T cells inhibited  
200 tumor cell outgrowth and eradicated the tumor before clinical manifestation (Figure 1B); 2) effector T  
201 cells were initially unable to inhibit tumor cell outgrowth, but caught up and suppressed tumor growth  
202 to a balanced subclinical state (Figure 1C); or 3) exponential tumor growth outpaced the immune  
203 system’s control and gave rise to a clinically detectable tumor (Figure 1D). These three scenarios only  
204 led to two clinically different outcomes in patients: either a tumor became clinically evident, or the  
205 immune system could suppress/eradicate a tumor at an early stage. A balanced equilibrium state, in  
206 which the immune system keeps a clinically evident tumor under persistent control, does not exist in  
207 this deterministic version of our model.

208

### 209 **Patient survival depends on a tipping point in tumor-immune dynamics**

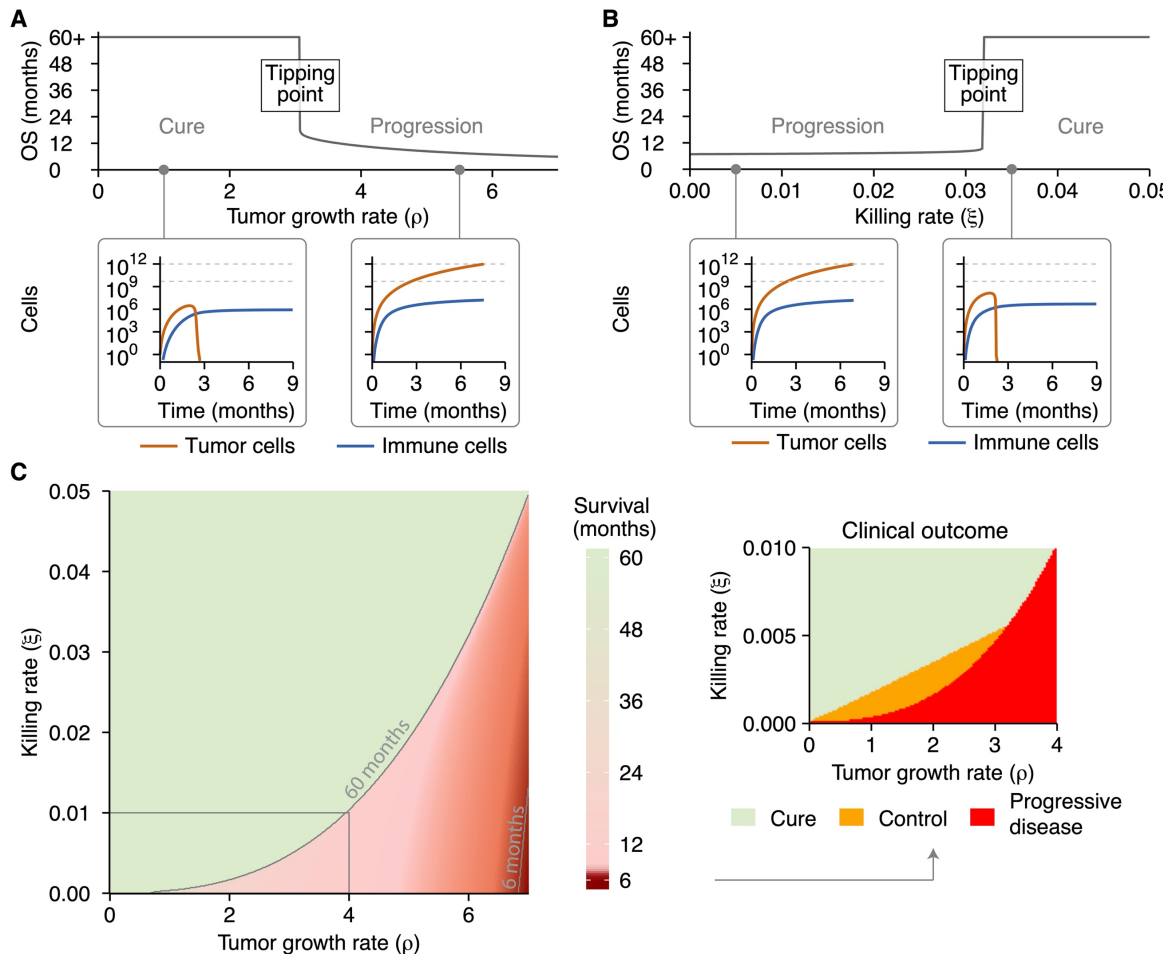
210 To better characterize these dichotomous survival kinetics, we examined how tumor-immune  
211 dynamics influenced patient survival by varying the tumor growth rate and the T cell killing rate over  
212 a broad range of possible values.

213 First, we focused solely on the tumor-component by varying the tumor growth rate. An increase in  
214 tumor growth did not gradually shorten overall survival in patients (Figure 2A). On the contrary, a  
215 critical threshold was present. Once the threshold was exceeded, the kinetics ‘flip’ from a state of  
216 immune control (Figure 2A, inset 1) to a state in which the tumor could evade immune control (Figure  
217 2A, inset 2).

218 Second, we investigated the influence of the T cell killing rate on overall survival. As for the death rate,  
219 a gradual increase in the cytotoxic capacity of effector T cells did not induce a gradual change in survival  
220 times. Instead, a sharp state transition was again observed that differentiated short from long survival  
221 (Figure 2B). This coincided with the phenotypes ‘immune evasion’ and ‘immune control’.

222 To visualize this sudden state transition or ‘tipping point’ in tumor-immune dynamics as a function of  
223 both tumor proliferation and cytotoxic killing at the same time, we visualized the joint influence of the  
224 tumor growth rate and T cell killing rate on survival in a heatmap (Figure 2C). This ‘phase diagram’  
225 shows that the tipping point is not only present for specific parameter values but is a fundamental  
226 property in our model. By contrast, the state of subclinical tumor control was not universally present  
227 around the tipping point (Figure 2C, inset) but manifested itself only in a narrow range of parameters.  
228 Nevertheless, the general presence of a tipping point indicates that small perturbations in either tumor  
229 growth rate or T cell killing rate in the vicinity of a tipping point may result in substantial overall survival

230 differences in patients, whereas much larger perturbations far away from the tipping point would have  
 231 far less effect.



232

**Figure 2: A tipping point in the tumor-immune interaction determines a patient's outcome.**

233 (A) A gradual increase in tumor growth reveals a tipping point, where long-term survival (immune control; inset 1) abruptly  
 234 changes to short-term survival (immune evasion; inset 2). (B) A similar analysis reveals a tipping point along the immune axis,  
 235 again differentiating short-term survival (immune evasion; inset 1) from long-term benefit (immune control; inset 2). (C) The  
 236 tipping point is present across the entire range of parameters examined. Cure and progressive disease are the dominant states,  
 237 whereas subclinical tumor control only occurs within a limited parameter range (inset). Simulation parameters are shown in  
 238 Supplementary Table 2.

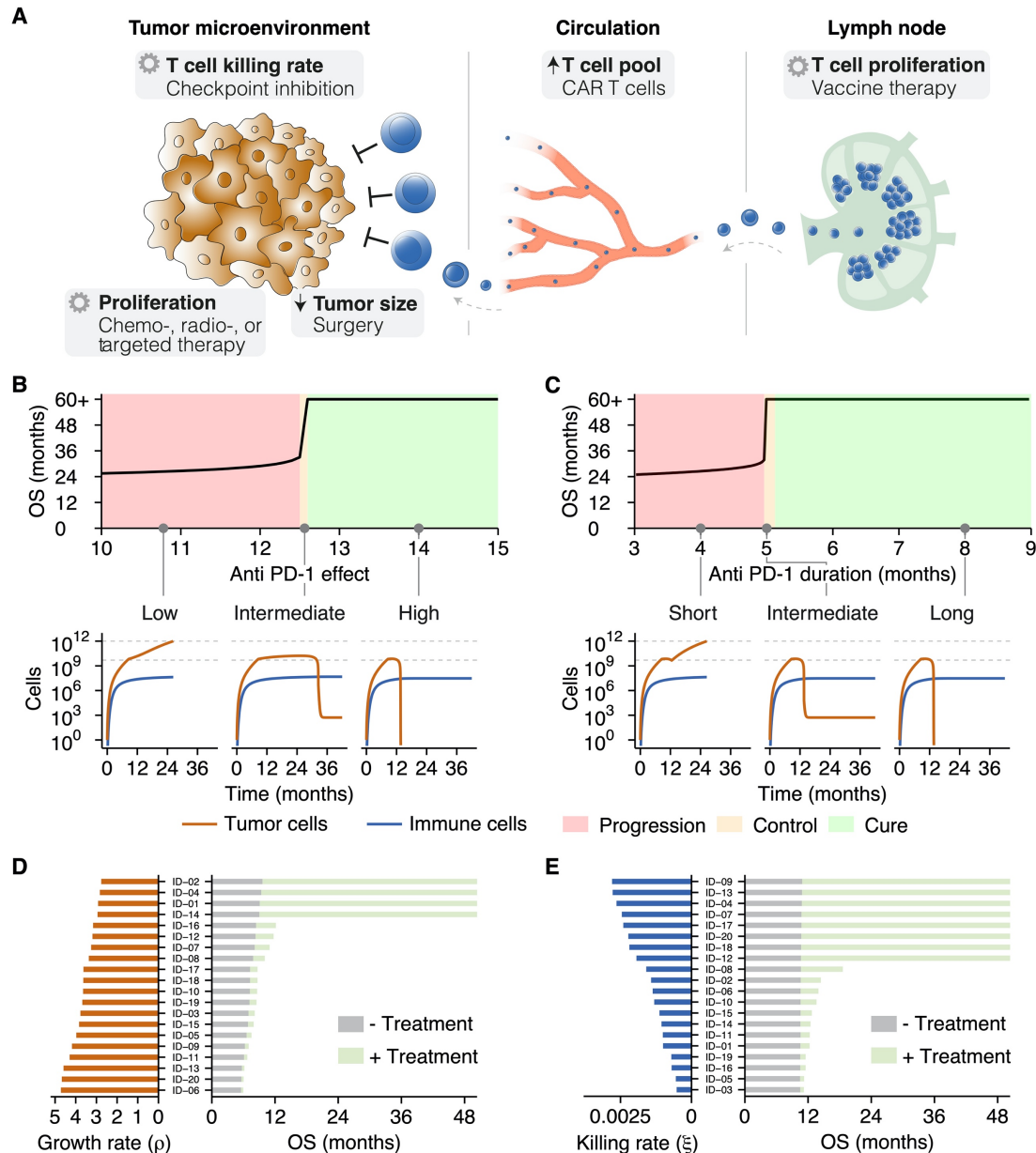
239

240

## 241 Immune checkpoint inhibitors induce a survival benefit by shifting patients over a tipping 242 point

243 So far, we have described tumor-immune interactions during the natural course of malignant disease.  
 244 In a clinical setting, however, therapeutic interventions are available to steer disease courses.  
 245 Dependent on the treatment of choice, a specific effect is exerted on the tumor microenvironment.  
 246 Treatment effects vary from constraining the proliferative capacity of tumor cells (e.g., chemotherapy  
 247 or targeted therapy) to increasing the T cell pool (e.g., CAR T cells) or expanding the proliferative  
 248 capacity of T cells (e.g., cancer vaccines; Figure 3A). Given the unparalleled responses of advanced  
 249 malignancies to immunotherapy, we focused on the consequences of a tipping point for responses to

250 immune checkpoint inhibitors (ICI), but these findings could be extended to other therapies as well. In  
 251 this study, we limited the treatment effect of ICI to their primary mode of action: the augmentation of  
 252 the T cell killing rate (Figure 3A).



253  
 254 **Figure 3: Tipping points induce dichotomous clinical outcomes in heterogeneous patient populations.**  
 255 (A) Treatments target processes or cell populations in the tumor microenvironment. (B-C) Two criteria need to be met to  
 256 induce long-term survival: (B) ICI need to augment T cell killing sufficiently, and (C) the treatment effect needs to be retained  
 257 for a prolonged time. An inadequate treatment effect or limited treatment duration led at maximum to a temporary survival  
 258 benefit. (D-E) In patient populations with variation in only (D) the tumor (i.e., growth rate), or (E) the immune system (i.e., T  
 259 cell killing rate), the distance to a tipping point determines the clinical benefit. Without treatment, survival was limited (grey  
 260 bars). In contrast, ICI induced long-term survival solely in patients close to a tipping point (green bars). See also Supplementary  
 261 Table 3.

262  
 263 In the presence of a tipping point, ICI could induce a long-term survival benefit under two conditions:  
 264 1) the effect of treatment needs to be potent enough to shift a patient over a tipping point (Figure 3B),  
 265 and 2) the treatment effect needs to be sustained long enough for a patient to benefit from the

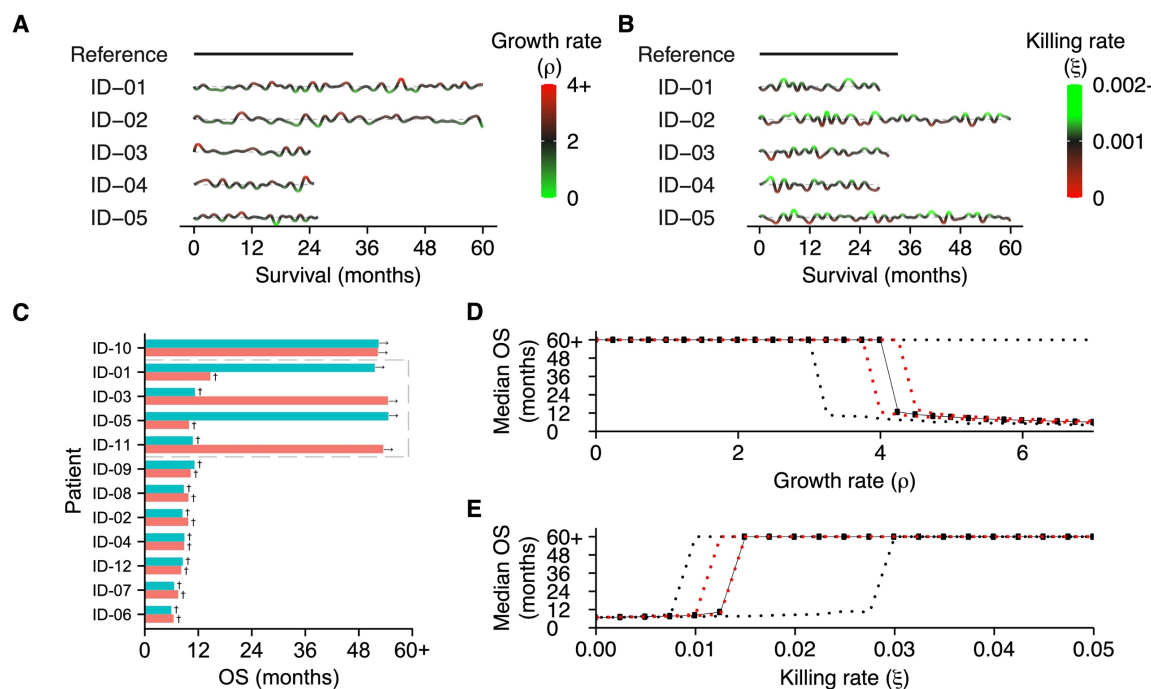
266 treatment (Figure 3C). The treatment effect is defined as the multiplication factor of the T cell killing  
267 rate. When both criteria were satisfied, ICI were able to induce a long-term survival benefit. However,  
268 if the treatment effect (anti-PD1 effect < 12.6) or duration (less than  $\pm 5$  months) proved inadequate,  
269 any survival benefit was only temporary, and inevitable tumor progression would ultimately limit  
270 overall survival (Figure 3B/C; insets). These survival kinetics depend not solely on therapeutic features  
271 of ICI but rather on the interplay between patient and ICI characteristics. To illustrate this, we  
272 simulated twenty patients with identical immune systems (i.e., identical T cell killing rates). In the  
273 absence of ICI therapy, variation in the tumor growth rate – that is, variation in the distance to a tipping  
274 point – led to a limited variation in survival (Figure 3D; grey bars). When these same patients were  
275 treated with ICI, a survival benefit is induced in all patients. However, the extent of this benefit differs  
276 and is dependent on the distance to a tipping point. Following clinical observations, long-term survival  
277 is only induced in the subset of patients close to a tipping point (Figure 3D; green bars). Similar findings  
278 were obtained in a population of patients with identical tumors but different immune systems.  
279 Without treatment, hardly any survival variation is present (Figure 3E; grey bars). Again, treatment  
280 with ICI induced dichotomous clinical outcomes: a small survival benefit in most patients, with long-  
281 term survival in a subset (Figure 3E; green bars). Hence, the mere presence of a tipping point yields  
282 heterogeneity in treatment outcomes.

283

#### 284 **Tipping points determine patient outcomes in dynamic patient trajectories**

285 Thus far, our simulations considered tipping points generated in patients with fixed characteristics.  
286 However, disease courses in patients are certainly not fixed and are, to a certain extent, subject to  
287 (random) variation. We hypothesized that interpatient variability in clinical outcomes could be  
288 (partially) attributable to this dynamic behavior of cancers and the interaction with the immune  
289 system. Such variation might reflect biological processes (e.g., accumulating mutations, the expression  
290 of checkpoint molecules, and the availability of nutrients) that alter anti-tumor immunity and promote  
291 or hamper tumor development. We reasoned that the subsequent dynamics could drive patients  
292 towards and ultimately over a tipping point – or move patients away from it, which would limit the  
293 survival benefit of these treatments. To verify this hypothesis, we simulated the effect of dynamically  
294 evolving tumors (Figure 4A) or immune systems (Figure 4B) in identical patients compared to a static  
295 reference patient. Specifically, we varied the tumor growth rate and the T cell killing rate randomly  
296 over time (parameter values are included in Supplementary Table 4). Upon reaching a diagnosable  
297 tumor volume, all patients in these examples were treated with ICI. As expected, stochastic dynamics  
298 prompted survival differences and induced a survival benefit in a subset of patients. In a  
299 heterogeneous patient population, this led to an interesting finding: the initial distance to a tipping

300 point, along with the dynamics itself, determined the clinical outcome of patients treated with ICI  
 301 (Figure 4C, Supplementary Figure 1). At population level, this led to a distinction between three subsets  
 302 of patients: (1) patients far away from a tipping point with an unmodifiable bad prognosis (non-  
 303 responders), (2) patients close to a tipping point with a favorable prognosis (responders), and, most  
 304 importantly, (3) patients in between these groups (potential responders). In the last subset, tumor  
 305 dynamics ultimately determined the treatment response, and thereby the clinical outcome (Figure 4C;  
 306 grey box). A clinically important ramification of dynamic trajectories is that even if the subset to which  
 307 a patient belongs is known at baseline, dynamics could alter the distance to a tipping point and,  
 308 thereby, the prognosis of a patient. Therefore, it might be impossible to predict the prognosis solely  
 309 based on characteristics measured upon diagnosis. Dynamic trajectories can significantly diversify  
 310 patient outcomes, meaning that continuous variation in the tumor growth rate (Figure 4D) or T cell  
 311 killing rate (Figure 4E) leads to an entire spectrum of patient outcomes.



312

**Figure 4: Survival outcomes are strongly affected by evolving patient dynamics.**

(A-B) Examples of dynamic disease courses in patients with identical tumors and immune systems at baseline, respectively. (A) Evolving tumors (i.e., random variation in tumor growth rate over time) and (B) continuous variation in the potency of the immune system (i.e., killing rate) lead to divergent survival outcomes. The grey dotted line indicates the baseline values for the growth rate and killing rate, respectively. (C) Dynamic trajectories in a heterogeneous patient population can move patients towards or away from a tipping point. The grey box indicates patients in which dynamic trajectories strongly alter survival outcomes. See also Supplementary Figure 1. In dynamic trajectories, (D) baseline tumor growth and (E) baseline T cell killing rates cannot accurately predict overall survival. Note: all patients in these examples are treated with ICI. The red and black dotted lines indicate the 25% and 75% quantiles, respectively. See also Supplementary Table 4.

322

323

324

325

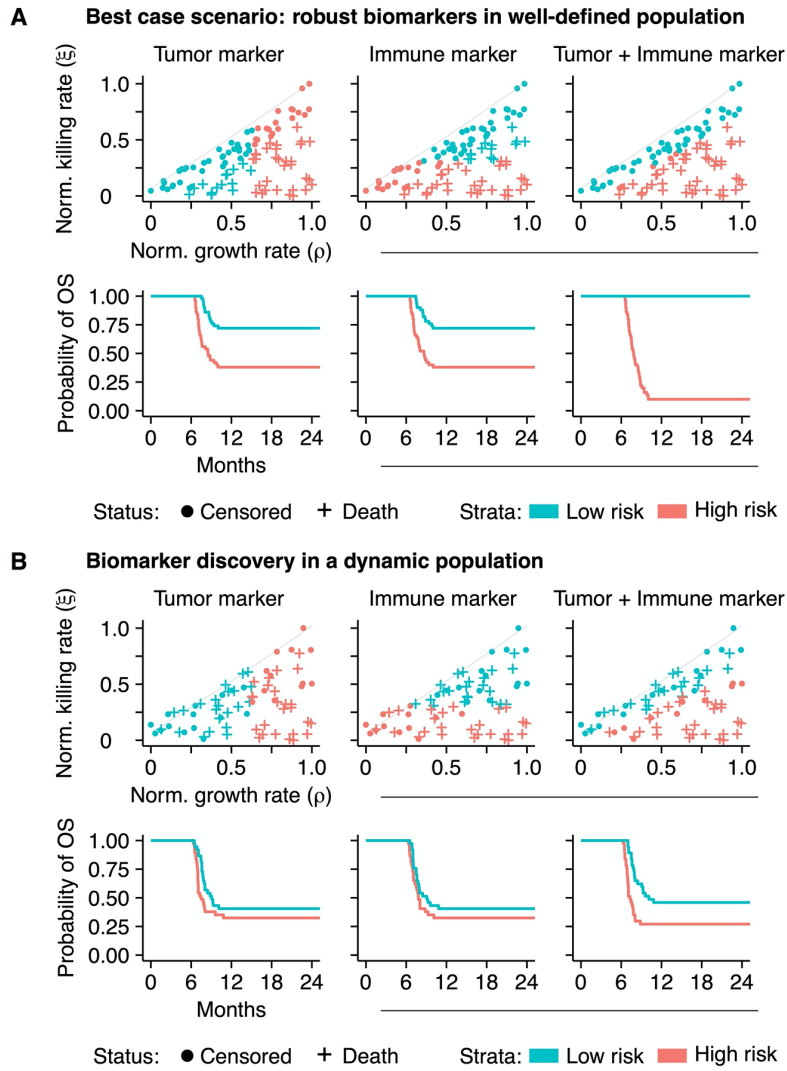
326 **Implications of tipping points for biomarker discovery studies**

327 Biomarker discovery studies aim to improve the prediction of patient survival upon treatment. We  
328 observed that tipping points are crucial in shaping survival kinetics. Therefore, accurate survival  
329 predictions would require the consideration of tipping points. Ideally, a prognostic biomarker (or  
330 biomarker panel) would consistently distinguish long-term survivors from their counterparts. Since the  
331 non-linear survival dynamics following a tipping point weaken the correlation between a single  
332 biomarker and survival, the question is: how can we screen for biomarkers in a more efficient manner  
333 that takes this tipping point into account?

334 We approached this question with an *in silico* biomarker discovery study. We measured the value of  
335 two potential biomarkers at baseline in patients (n=100) that were subsequently treated with ICI. We  
336 simplified the cohort by fixing the tumor and immune characteristics of these patients over time and  
337 assumed to have access to an entirely accurate biomarker (i.e., no measurement error; Figure 5A).  
338 Within this cohort, we predicted the prognosis of patients based on either the tumor or immune  
339 marker (the first and second columns of Figure 5A, respectively). As is common in practice (though  
340 from a statistical point of view far from ideal), we dichotomized the biomarker using its median as a  
341 cut-off. Although survival differentiation based on these biomarkers alone was partially possible, it  
342 remained far from optimal. However, when we constructed a biomarker panel including both  
343 biomarkers, it highly accurately discriminated short-term from long-term survivors (third column of  
344 Figure 5A, Supplementary information). Note that despite variability in time from diagnosis, the initial  
345 plateau in the survival curves was caused by the fact that all tumors were diagnosed with identical  
346 sizes and immediately treated.

347 In clinical practice, the assumption of a ‘fixed’ patient trajectory does not hold. Therefore, we  
348 simulated this cohort again with dynamic trajectories. Due to the dynamics, a subgroup of patients did  
349 not develop clinical tumors and was excluded from the analysis. The prediction of a patient’s prognosis  
350 with a single biomarker, either from the tumor or the immune system, in a dynamic cohort became  
351 increasingly challenging (the first and second columns of Figure 5B). The combination of both markers  
352 in a biomarker panel increased the predictive capacity slightly, enabling the prediction of prognosis to  
353 some extent. However, in line with the notion of personalized medicine, the accurate and  
354 individualized prediction of prognosis based on baseline characteristics was not feasible in a significant  
355 subgroup of patients due to dynamic tumor-immune interactions (third column of Figure 5B). Two  
356 important findings are derived from these observations: First, due to the non-linear tumor-immune  
357 dynamics with respect to survival, it is highly unlikely that a single biomarker can accurately predict a  
358 patients’ prognosis. Since survival kinetics emerge from the interplay between a cancer and the  
359 immune system, biomarkers from both systems need to be incorporated simultaneously into a  
360 biomarker panel to improve the predictive value. Second, biomarker measurements at baseline are

361 merely a situational snapshot of the disease conditions *at a specific point in time*. Depending on the  
362 magnitude of the dynamics, it might become challenging or even impossible to correctly predict the  
363 prognosis of patients from these biomarkers, stressing the need for continuous monitoring.



364 Status: ● Censored + Death Strata: ■ Low risk ■ High risk

365 **Figure 5: Non-linear tumor-immune dynamics complicate biomarker discovery.**  
366 (A) An *in silico* biomarker discovery study in a ‘fixed’ patient cohort: while a single biomarker – either a tumor or an immune  
367 marker – can predict survival to some extent (the first and second columns), information from both markers in a biomarker  
368 panel enhances the predictive capacity greatly (third column). (B) Dynamic disease trajectories challenge survival prediction  
369 with ‘baseline’ biomarkers and stress the need for continuous monitoring. Disease dynamics challenge the predictive value of  
370 single ‘baseline’ biomarkers (the first and second columns; compare to Figure 5A). A biomarker panel improves survival  
371 predictions in this cohort (the third column) but is still defied by evolving dynamics. See also Supplementary figure 5.

372

## 373 DISCUSSION

374 This study investigated how tumor-immune dynamics relate to ICI-induced treatment responses and  
375 survival kinetics of patients. We predict that a tipping point is present in the tumor-immune  
376 interaction. This finding implies that at the basis of the intricate interplay between a developing  
377 malignancy and the immune system contrasting disease states determine disease outcome: a state  
378 where the immune system controls tumor outgrowth and a state in which a tumor escapes immune

379 defense. A stable “steady state” in which tumor growth and the immune response perfectly balance  
380 each other for extended periods seems only plausible in a subclinical setting. We show that treatment  
381 with ICI can induce a survival benefit by shifting a patient over a tipping point, thereby tipping the  
382 balance in tumor-immune dynamics in favor of survival. In line with clinical observations of interpatient  
383 variability in disease courses, we found that dynamics in patient trajectories might contribute to  
384 unpredictability in treatment responses. Moreover, we showed how the tipping point in dynamic  
385 patient trajectories defies simple strategies for outcome prediction in biomarker discovery studies,  
386 stressing the need for advanced mechanism-based monitoring.

387 Tipping points are well-known in complex systems such as financial markets and ecosystems but are  
388 also present in medicine (44, 45). State transitions might progress gradually or abruptly. If a system  
389 balances around a critical threshold, small perturbations might induce an abrupt transition to a  
390 contrasting state. In oncology, phenomena as partial or complete radiologic responses during  
391 treatment or (hyper)progression after discontinuation of treatment suggest the presence of state  
392 transitions (46, 47). Based on these observations, a tipping point in cancer immunotherapy had been  
393 speculated upon (48). Experimentally, tipping points are most clearly represented by early preclinical  
394 work in the PD-1/PD-L1 axis. Consistent with our findings, dichotomous treatment responses arise in  
395 syngeneic DBA/2 mice inoculated with P815/PD-L1 cells (49). While genetically identical with similar  
396 tumor characteristics, anti-PD-L1 antibodies could prolong survival in only a subset of the mice, likely  
397 due to stochastic differences in immune responses and TCR repertoire. Additional *in vivo* data  
398 supporting the theory of tipping points in oncology is derived from studies on dynamic network  
399 biomarkers, showing its relevance during the onset of metastasis in hepatocellular carcinoma (50) and  
400 the development of treatment resistance in breast cancer (51). This study provides a potential  
401 mechanistic explanation for this phenomenon in immuno-oncology and shows its implications on the  
402 induction of long-term survival in clinical practice and biomarker discovery. From a biomechanistic  
403 perspective, such state transitions in cancer immunotherapy arise due to fundamental differences in  
404 proliferation kinetics between tumors and the immune system. While tumor cell proliferation is  
405 virtually unrestricted, immune cell proliferation is much more limited and tightly controlled. Our  
406 finding that tipping points affect not only natural disease courses but also treatment responses  
407 underlines the importance of these kinetics.

408 An important implication of tipping points within tumor-immune dynamics involves biomarker  
409 discovery. Biomarkers are developed to predict prognosis and steer clinical decision making. Disease  
410 outcomes in cancer patients are essentially determined by the interplay between two complex  
411 systems: the tumor and the immune system. Our model predicts that factors from both systems should  
412 be considered to improve the predictive power of biomarkers. However, in contrast with this  
413 seemingly straightforward prediction, current research mainly focuses on factors derived from one of

414 the two complex systems. Expression of programmed death ligand-1 (PD-L1) on tumor tissue illustrates  
415 this properly: while 45% of patients with PD-L1 positive tumors show objective responses to anti-  
416 PD(L)1 immunotherapy, 15% of patients with PD-L1 negative tumors also show objective responses  
417 (52). Other explanations for this difference include heterogeneous intratumoral and inter-metastases  
418 expression patterns, positivity-threshold selection, and differences in immunohistochemical staining  
419 protocols. In that respect, tumor mutational burden (TMB) might prove to be a highly relevant  
420 biomarker. The mutation rate is a tumor-intrinsic factor associated with the phenotypical  
421 aggressiveness of tumors (53). Simultaneously, a high mutational burden might induce a plethora of  
422 neoantigens, linking this tumor-intrinsic factor directly to adaptive immunity. Clinical observations of  
423 a stronger association between TMB and response rates to anti-PDL1 immunotherapy compared to  
424 PD-L1 expression in patients with urothelial carcinoma support this hypothesis (54). Thus, reinforcing  
425 common calls to integrate multiple existing biomarkers for immunotherapy prediction outcomes (55,  
426 56), our research indicates that a combination of both immunological and tumor-related parameters  
427 should be the basis of *any* biomarker discovery effort. The strongly non-linear dynamics resulting from  
428 the tipping point mean that a one-dimensional approach will likely be insufficient.

429 Our approach has to be interpreted in light of some limitations. Although the ‘coarse-grained’ nature  
430 of ODE models allows focusing on the major common underlying mechanisms in many cancers, it is  
431 also a potential pitfall. For example, metabolic processes such as hypoxia, immune-suppressive  
432 characteristics of the tumor microenvironment such as the presence of FoxP3<sup>+</sup> regulatory T cells or  
433 expression of transforming growth factor  $\beta$ , the presence of additional relevant effector cells such as  
434 natural killer cells, and the availability of nutrients are only implicitly represented by our model in a  
435 single killing efficacy parameter. This simplification also holds for treatments. In this study, ICI was  
436 limited to its main mode of action: the augmentation of the T cell killing rate. While the ‘true’  
437 mechanistic effects might be more widespread, sufficient data to correctly parameterize more  
438 complex models remains scarce. Furthermore, it should be emphasized that an ODE model contains  
439 limited spatial information; while we distinguish between lymphatic tissue and the tumor  
440 microenvironment, all cells within the microenvironment are identical, and all processes affect cells in  
441 the same manner. We do not expect that explicit incorporation of these processes or translation of  
442 the model into a spatial variant alters our findings of a tipping point; however, it might be of interest  
443 to verify these hypotheses in future research in spatial agent-based models.

444 In conclusion, we used a computational modeling approach to show that the clinical outcome of cancer  
445 patients is determined by tipping points in tumor-immune dynamics. A tipping point influences not  
446 only response to treatment but also the prognosis of patients and has major implications for future  
447 biomarker research.

448

449 **REFERENCES**

- 450 1. Larkin J, Chiarion-Sileni V, Gonzalez R, et al. Five-Year Survival with Combined Nivolumab and  
451 Ipilimumab in Advanced Melanoma. *N Engl J Med.* 2019;381(16):1535-46.
- 452 2. Hellmann MD, Paz-Ares L, Bernabe Caro R, et al. Nivolumab plus Ipilimumab in Advanced Non-  
453 Small-Cell Lung Cancer. *N Engl J Med.* 2019;381(21):2020-31.
- 454 3. Motzer RJ, Escudier B, McDermott DF, et al. Survival outcomes and independent response  
455 assessment with nivolumab plus ipilimumab versus sunitinib in patients with advanced renal cell  
456 carcinoma: 42-month follow-up of a randomized phase 3 clinical trial. *J Immunother Cancer.* 2020;8(2).
- 457 4. Aly A, Mullins CD, Hussain A. Understanding heterogeneity of treatment effect in prostate  
458 cancer. *Curr Opin Oncol.* 2015;27(3):209-16.
- 459 5. Kent DM, Alsheikh-Ali A, Hayward RA. Competing risk and heterogeneity of treatment effect  
460 in clinical trials. *Trials.* 2008;9:30.
- 461 6. Bedard PL, Hansen AR, Ratain MJ, et al. Tumour heterogeneity in the clinic. *Nature.*  
462 2013;501(7467):355-64.
- 463 7. Dagogo-Jack I, Shaw AT. Tumour heterogeneity and resistance to cancer therapies. *Nat Rev  
464 Clin Oncol.* 2018;15(2):81-94.
- 465 8. Sharma P, Hu-Lieskov S, Wargo JA, et al. Primary, Adaptive, and Acquired Resistance to  
466 Cancer Immunotherapy. *Cell.* 2017;168(4):707-23.
- 467 9. Roskoski R, Jr. A historical overview of protein kinases and their targeted small molecule  
468 inhibitors. *Pharmacol Res.* 2015;100:1-23.
- 469 10. Kern SE. Why your new cancer biomarker may never work: recurrent patterns and remarkable  
470 diversity in biomarker failures. *Cancer Res.* 2012;72(23):6097-101.
- 471 11. Murphy H, Jaafari H, Dobrovolsky HM. Differences in predictions of ODE models of tumor  
472 growth: a cautionary example. *BMC Cancer.* 2016;16:163.
- 473 12. Edelman EJ, Guinney J, Chi JT, et al. Modeling cancer progression via pathway dependencies.  
474 *PLoS Comput Biol.* 2008;4(2):e28.
- 475 13. Baratchart E, Benzekry S, Bikfalvi A, et al. Computational Modelling of Metastasis Development  
476 in Renal Cell Carcinoma. *PLoS Comput Biol.* 2015;11(11):e1004626.
- 477 14. De Mattos-Arruda L, Vazquez M, Finotello F, et al. Neoantigen prediction and computational  
478 perspectives towards clinical benefit: recommendations from the ESMO Precision Medicine Working  
479 Group. *Ann Oncol.* 2020;31(8):978-90.
- 480 15. Pujana MA, Han JD, Starita LM, et al. Network modeling links breast cancer susceptibility and  
481 centrosome dysfunction. *Nat Genet.* 2007;39(11):1338-49.
- 482 16. Friberg LE, Henningsson A, Maas H, et al. Model of chemotherapy-induced myelosuppression  
483 with parameter consistency across drugs. *J Clin Oncol.* 2002;20(24):4713-21.
- 484 17. Lee JJ, Huang J, England CG, et al. Predictive modeling of in vivo response to gemcitabine in  
485 pancreatic cancer. *PLoS Comput Biol.* 2013;9(9):e1003231.
- 486 18. Wang HW, Milberg O, Bartelink IH, et al. In silico simulation of a clinical trial with anti-CTLA-4  
487 and anti-PD-L1 immunotherapies in metastatic breast cancer using a systems pharmacology model.  
488 *Roy Soc Open Sci.* 2019;6(5).
- 489 19. Valentiniuzzi D, Simoncic U, Ursic K, et al. Predicting tumour response to anti-PD-1  
490 immunotherapy with computational modelling. *Phys Med Biol.* 2019;64(2):025017.
- 491 20. Sun X, Bao J, Shao Y. Mathematical Modeling of Therapy-induced Cancer Drug Resistance:  
492 Connecting Cancer Mechanisms to Population Survival Rates. *Sci Rep.* 2016;6:22498.
- 493 21. Zhang J, Cunningham JJ, Brown JS, et al. Integrating evolutionary dynamics into treatment of  
494 metastatic castrate-resistant prostate cancer. *Nat Commun.* 2017;8(1):1816.
- 495 22. Cunningham JJ, Brown JS, Gatenby RA, et al. Optimal control to develop therapeutic strategies  
496 for metastatic castrate resistant prostate cancer. *J Theor Biol.* 2018;459:67-78.
- 497 23. Ribba B, Boetsch C, Nayak T, et al. Prediction of the Optimal Dosing Regimen Using a  
498 Mathematical Model of Tumor Uptake for Immunocytokine-Based Cancer Immunotherapy. *Clin Cancer  
499 Res.* 2018;24(14):3325-33.

- 500 24. Fassoni AC, Baldow C, Roeder I, et al. Reduced tyrosine kinase inhibitor dose is predicted to be  
501 as effective as standard dose in chronic myeloid leukemia: a simulation study based on phase III trial  
502 data. *Haematologica*. 2018;103(11):1825-34.
- 503 25. Clark RE, Polydoros F, Aupperley JF, et al. De-escalation of tyrosine kinase inhibitor therapy  
504 before complete treatment discontinuation in patients with chronic myeloid leukaemia (DESTINY): a  
505 non-randomised, phase 2 trial. *Lancet Haematol*. 2019;6(7):e375-e83.
- 506 26. Mendelsohn ML. Cell proliferation and tumor growth. *Oxford: Blackwell Scientific Publications*.  
507 1963.
- 508 27. Borghans JA, de Boer RJ, Segel LA. Extending the quasi-steady state approximation by changing  
509 variables. *Bull Math Biol*. 1996;58(1):43-63.
- 510 28. Gadhamsetty S, Maree AF, Beltman JB, et al. A general functional response of cytotoxic T  
511 lymphocyte-mediated killing of target cells. *Biophys J*. 2014;106(8):1780-91.
- 512 29. McDonagh M, Bell EB. The survival and turnover of mature and immature CD8 T cells.  
513 *Immunology*. 1995;84(4):514-20.
- 514 30. Jenkins MK, Chu HH, McLachlan JB, et al. On the composition of the preimmune repertoire of  
515 T cells specific for Peptide-major histocompatibility complex ligands. *Annu Rev Immunol*. 2010;28:275-  
516 94.
- 517 31. Coulie PG, Karanikas V, Lurquin C, et al. Cytolytic T-cell responses of cancer patients vaccinated  
518 with a MAGE antigen. *Immunol Rev*. 2002;188:33-42.
- 519 32. Westermann J, Pabst R. Distribution of lymphocyte subsets and natural killer cells in the human  
520 body. *Clin Investig*. 1992;70(7):539-44.
- 521 33. Ferrer R. Lymphadenopathy: differential diagnosis and evaluation. *Am Fam Physician*.  
522 1998;58(6):1313-20.
- 523 34. Vallini V, Ortori S, Boraschi P, et al. Staging of pelvic lymph nodes in patients with prostate  
524 cancer: Usefulness of multiple b value SE-EPI diffusion-weighted imaging on a 3.0 T MR system. *Eur J  
525 Radiol Open*. 2016;3:16-21.
- 526 35. Linderman JJ, Riggs T, Pande M, et al. Characterizing the dynamics of CD4+ T cell priming within  
527 a lymph node. *J Immunol*. 2010;184(6):2873-85.
- 528 36. Drake CG, Jaffee E, Pardoll DM. Mechanisms of immune evasion by tumors. *Adv Immunol*.  
529 2006;90:51-81.
- 530 37. Halle S, Halle O, Forster R. Mechanisms and Dynamics of T Cell-Mediated Cytotoxicity In Vivo.  
531 *Trends Immunol*. 2017;38(6):432-43.
- 532 38. Beck RJ, Slagter M, Beltman JB. Contact-Dependent Killing by Cytotoxic T Lymphocytes Is  
533 Insufficient for EL4 Tumor Regression In Vivo. *Cancer Res*. 2019;79(13):3406-16.
- 534 39. Del Monte U. Does the cell number 10(9) still really fit one gram of tumor tissue? *Cell Cycle*.  
535 2009;8(3):505-6.
- 536 40. Moreno CC, Mittal PK, Sullivan PS, et al. Colorectal Cancer Initial Diagnosis: Screening  
537 Colonoscopy, Diagnostic Colonoscopy, or Emergent Surgery, and Tumor Stage and Size at Initial  
538 Presentation. *Clin Colorectal Cancer*. 2016;15(1):67-73.
- 539 41. Zastrow S, Phuong A, von Bar I, et al. Primary tumor size in renal cell cancer in relation to the  
540 occurrence of synchronous metastatic disease. *Urol Int*. 2014;92(4):462-7.
- 541 42. Ball DL, Fisher RJ, Burmeister BH, et al. The complex relationship between lung tumor volume  
542 and survival in patients with non-small cell lung cancer treated by definitive radiotherapy: a  
543 prospective, observational prognostic factor study of the Trans-Tasman Radiation Oncology Group  
544 (TROG 99.05). *Radiother Oncol*. 2013;106(3):305-11.
- 545 43. Ahnert K, Mulansky M. Odeint – Solving Ordinary Differential Equations in C++. *AIP Conference  
546 Proceedings*. 2011;1389.
- 547 44. Scheffer M, Carpenter SR, Lenton TM, et al. Anticipating critical transitions. *Science*.  
548 2012;338(6105):344-8.
- 549 45. Scheffer M, Bascompte J, Brock WA, et al. Early-warning signals for critical transitions. *Nature*.  
550 2009;461(7260):53-9.

- 551 46. Eisenhauer EA, Therasse P, Bogaerts J, et al. New response evaluation criteria in solid tumours:  
552 revised RECIST guideline (version 1.1). *Eur J Cancer*. 2009;45(2):228-47.
- 553 47. Champiat S, Dercle L, Ammari S, et al. Hyperprogressive Disease Is a New Pattern of  
554 Progression in Cancer Patients Treated by Anti-PD-1/PD-L1. *Clin Cancer Res*. 2017;23(8):1920-8.
- 555 48. Lesterhuis WJ, Bosco A, Millward MJ, et al. Dynamic versus static biomarkers in cancer immune  
556 checkpoint blockade: unravelling complexity. *Nat Rev Drug Discov*. 2017;16(4):264-72.
- 557 49. Iwai Y, Ishida M, Tanaka Y, et al. Involvement of PD-L1 on tumor cells in the escape from host  
558 immune system and tumor immunotherapy by PD-L1 blockade. *Proc Natl Acad Sci U S A*.  
559 2002;99(19):12293-7.
- 560 50. Yang B, Li M, Tang W, et al. Dynamic network biomarker indicates pulmonary metastasis at the  
561 tipping point of hepatocellular carcinoma. *Nat Commun*. 2018;9(1):678.
- 562 51. Liu R, Wang J, Ukai M, et al. Hunt for the tipping point during endocrine resistance process in  
563 breast cancer by dynamic network biomarkers. *J Mol Cell Biol*. 2019;11(8):649-64.
- 564 52. Sunshine J, Taube JM. PD-1/PD-L1 inhibitors. *Curr Opin Pharmacol*. 2015;23:32-8.
- 565 53. Thomas A, Routh ED, Pullikuth A, et al. Tumor mutational burden is a determinant of immune-  
566 mediated survival in breast cancer. *Oncoimmunology*. 2018;7(10):e1490854.
- 567 54. Balar AV, Galsky MD, Rosenberg JE, et al. Atezolizumab as first-line treatment in cisplatin-  
568 ineligible patients with locally advanced and metastatic urothelial carcinoma: a single-arm,  
569 multicentre, phase 2 trial. *Lancet*. 2017;389(10064):67-76.
- 570 55. Blank CU, Haanen JB, Ribas A, et al. CANCER IMMUNOLOGY. The "cancer immunogram".  
571 *Science*. 2016;352(6286):658-60.
- 572 56. Galon J, Pages F, Marinkola FM, et al. The immune score as a new possible approach for the  
573 classification of cancer. *J Transl Med*. 2012;10:1.
- 574
- 575

576 **LIST OF ABBREVIATIONS**

577 ICI: Immune Checkpoint Inhibition; ODE: Ordinary Differential Equation; PD-(L)1: Programmed Death-  
578 (Ligand) 1; TMB: Tumor Mutational Burden.

579

580 **DECLARATIONS**

581 **Ethics approval and consent to participate**

582 Not applicable.

583

584 **Consent for publication**

585 Not applicable.

586

587 **Availability of data and material**

588 The code of the ODE model is available at GitHub: <https://github.com/jeroencreemers/tipping-point->  
589 [cancer-immune-dynamics](https://github.com/jeroencreemers/tipping-point-cancer-immune-dynamics).

590

591 **Competing interests**

592 WJL reports consultancy activities for Douglas Pharmaceuticals and MSD; research funding from  
593 Douglas Pharmaceuticals, AstraZeneca, and ENA therapeutics; patents PCT/AU2019/050259 and

594 PCT/AU2015/000458 (all outside this work). NM reports personal fees from Bayer and Merck Sharp &  
595 Dohme; grants and personal fees from Jansen-Cilag, Roche, Astellas, and Sanofi (all outside this work).  
596 WRG reports consultancy activities for Bristol-Myers Squibb, IMS Health, Janssen-Cilag, Sanofi, and  
597 MSD; speaker fees from ESMO and MSD; and research funding from Bayer, Astellas, Janssen-Cilag, and  
598 Sanofi (all outside this work).

599

600 **Funding**

601 JC was funded by the Radboudumc. WJL was supported by Fellowships from the NHMRC, the Simon  
602 Lee Foundation, and the Cancer Council Western Australia. CF received an ERC Adv Grant ARTimmune  
603 (834618) and an NWO Spinoza grant. IV received an NWO-Vici grant (918.14.655). JT was supported  
604 by a Young Investigator Grant (10620) from the Dutch Cancer Society and an NWO grant  
605 (VI.Vidi.192.084).

606

607 **Authors' contribution**

608 JHAC and JT conceived this study. JHAC performed the experiments and wrote the manuscript under  
609 the supervision of JT. All authors provided feedback on the manuscript and reviewed the manuscript  
610 prior to submission.

611

612 **Acknowledgements**

613 Not applicable.